



Impact of ligand substituents on the crystal structures, optical and conducting properties of phenylmercury(II) β -oxodithioester complexes



Kavita Kumari^a, Michael G.B. Drew^b, Nanhai Singh^{a,*}

^a Department of Chemistry, Institute of Science, Banaras Hindu University, Varanasi 221005, India

^b Department of Chemistry, University of Reading, Whiteknights, Reading RG6 6AD, UK

ARTICLE INFO

Article history:

Received 9 August 2020

Revised 12 September 2020

Accepted 14 September 2020

Available online 25 September 2020

Keywords:

Conductivity

Crystal structures

PhHg(II) β -oxodithioesters

Luminescent properties

ABSTRACT

New phenylmercury(II) complexes **1–5** with functionalized β -oxodithioester ligands, [PhHg(II) (β -oxodithioester)], β -oxodithioester = methyl-3-hydroxy-3-(4-pyridyl)-2-propenedithioate L1 **1**, methyl-3-hydroxy-3-(*p*-chlorophenyl)-2-propenedithioate L2 **2**, methyl-3-hydroxy-3-(naphthyl)-2-propenedithioate L3 **3**, methyl-3-hydroxy-3-(9-anthracenyl)-2-propenedithioate L4 **4** and methyl-3-hydroxy-3-(*p*-fluorophenyl)-2-propenedithioate L5 **5**, were synthesized and characterized by elemental (C, H, N) analysis, IR, UV-Vis., ¹H and ¹³C{¹H} NMR spectroscopy. Their structures have been investigated by single crystal X-ray diffraction. Linear two-coordinate geometry about the Hg atom, via *ipso*-C of the phenyl group and by S15 atom of the β -oxodithioester ligands is revealed in all complexes. Intramolecular Hg...O bonding at 2.622(10)–2.813(6) Å is present in all the complexes. In **1–3**, the asymmetric unit contains a single discrete molecule whereas complexes **4** and **5** contain two. Except for **4** having bulky anthracene substituent, intriguing supramolecular networks are sustained through intermolecular metal assisted Hg...S and Hg...N and Cl...Cl, Cl... π , S...S, C–H...S, C–H...F, C–H... π interactions in these complexes. In **1** the pyridyl N on 4-position on the substituent is involved in Hg...N bonding interactions on the neighboring molecule at 2.938(7) Å generating a 2-D net-like polymeric structure. All the complexes showed bright green luminescent emissions both in solution and solid phase. The complexes (σ_{rt} values = 10^{−3}–10^{−6} S cm^{−1}) show semiconducting characteristics with Ea values = 0.14–0.64 eV. The electronic and steric properties of the substituents on the dithioester unit significantly influence their structures and properties.

© 2020 Elsevier B.V. All rights reserved.

1. Introduction

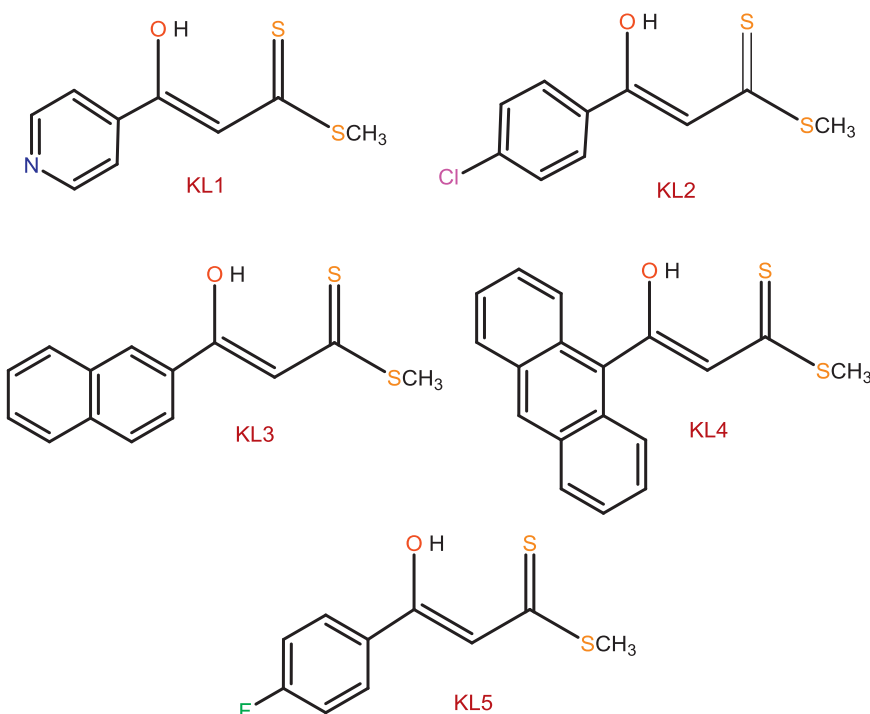
There has been significant growth of interest in the coordination chemistry of organomercury(II) and mercury(II) compounds not only to gain understanding concerning mercury-cysteine interactions in biological processes which can lead to severe health hazards causing damage to brain and endocrine system, environmental pollution and possible chemical antidotes, but also because of their intriguing structural chemistry and material properties [1–7]. The chemistry of metal complexes including mercury with 1,1-dithiolato ligands, such as dithiocarbamate, xanthate and dithiophosphate containing identical S,S-donor atoms have been widely explored because of their multifaceted chemistry and applications in diverse areas [8–17]. Metal complexes of related

dithioester ligands have been reported [18,19] but their structural investigations, study of properties and applications have gained little attention [20–22] although in recent years some main group and transition metal have been studied [20,21].

The developing interest in dithioester ligand chemistry is due to the functionalization of substituents that may substantially give rise to intriguing structures and modified physical properties. It is therefore crucial to make changes to ligand substituents with varied electronic and steric characteristics to map out the structures and properties of their complexes. With this in mind, in this contribution we report on the syntheses, crystal structures, luminescent and conducting properties of five new phenylmercury(II) complexes with pyridyl 4(N), *p*-chlorophenyl, 2-naphthyl, 9-anthracenyl and *p*-fluorophenyl functionalized β -oxodithioester ligands (Scheme 1). The important perspectives of pursuing this work are: (i) unlike 1,1-dithio ligands with soft bidentate S,S-donors, the β -oxodithioesters having both soft S and hard O donor atoms may expand their bonding ability with a variety of hard

* Corresponding author.

E-mail address: nsingh@bhu.ac.in (N. Singh).

**Scheme 1.** The β -oxodithioester ligands used in the work.

and soft metal ions. Usually the O,S-coordination mode of the β -oxodithioester ligands stabilize six-membered chelate ring in comparison to strained four-membered chelate rings formed by 1,1-dithio ligands about the metal centre; (ii) the compounds of mercury(II), with d^{10} electronic configuration do not feature ligand field bands and as a result their coordination numbers as well as structures are not imposed by ligand field stabilization requirements. The usual coordination numbers exhibited are 2 and 4 with linear/tetrahedral arrangements, however higher coordination numbers 3, 5 and 6 are also stabilized with weaker metal assisted bonding interactions. In-spite of the strength of Hg–S bond, the Hg...S and Hg...O interactions play crucial roles in the organization of supramolecular motifs. The incorporation of substituents on the dithioester backbone with varied steric bulk and different donor atoms N, Cl or F may induce secondary bonding interactions and increase the dimensionality of the complexes; (iii) the luminescent properties of divalent group 12 metal complexes particularly with Zn and Cd [5b,5d,23–26] are well documented, however studies on mercury complexes are rather scant. The more electronegative oxygen with small p-orbitals and less electronegative sulfur with more diffused d-orbitals within the molecules may modify the HOMO-LUMO gap and hence vary luminescent characteristics; and (iv) the sulfur rich planar metal complexes exhibited interesting conducting properties in solid state because of effective S...S intermolecular contacts [14–16]. The non planar complexes of chalcogenocyanates though limited in number, have also displayed interesting conducting characteristics [27,28].

2. Experimental

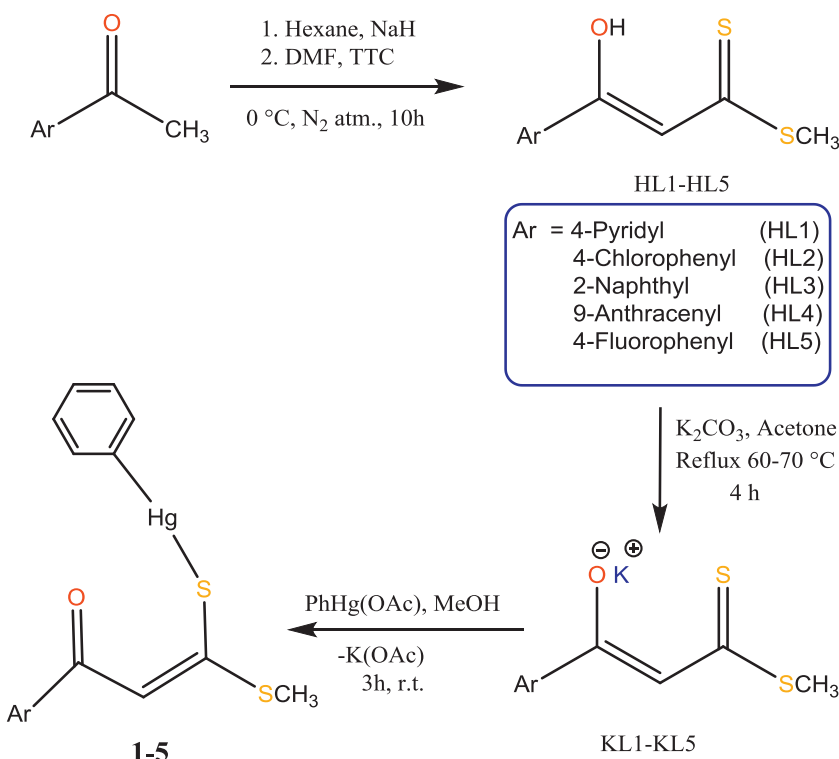
2.1. Materials and methods

All experiments were carried out in air at ambient temperature and pressure except the syntheses of ligands which were carried out under N_2 atmosphere. Reagent grade chemicals, PhHg(OAc) (SD Fine Chemicals), 4-acetylpyridine, 9-acylanthracene (SPEC-

TROCHEM), 2-acetylnaphthalene, *p*-chloroacetophenone and *p*-fluoroacetophenone (Avra) were procured and used as received. Solvents were purified and distilled adopting standard procedures [29]. Melting points of the complexes were measured in open capillaries using a Gallenkamps apparatus and are uncorrected. The experimental details dealing with the elemental analysis (C, H, N) and recording of IR (as KBr pellets) are the same as described earlier [21]. NMR (1H , $^{13}C\{^1H\}$) spectra were recorded on a JEOL ECZ500 MHz FT-NMR spectrometer in $CDCl_3$ [21b]. Chemical shifts were reported in ppm using TMS as internal standard. UV-Vis absorption, and solution and solid phase photoluminescent spectra were obtained at room temperature using Shimadzu UV-1800 and PerkinElmer LS-55 fluorescence spectrophotometer, respectively. The pressed pellet conductivity of the complexes was measured on a Keithley 236 Source Measure Unit by using a conventional two probe technique. X-ray powder diffraction data (PXRD) were collected on a Bruker D8 diffractometer with Cu $K\alpha$ radiation ($\lambda = 1.541836 \text{ \AA}$) in the 2θ range 5–50°, with a scan speed and a step size of 1° and 0.02° min⁻¹ respectively.

2.2. Synthesis of ligands (HL1–HL5)

The ligands, methyl-3-hydroxy-3-(4-pyridine)-2-propenedithioate HL1, methyl-3-hydroxy-3-(*p*-chlorophenyl)-2-propenedithioate HL2, methyl-3-hydroxy-3-(2-naphthyl)-2-propenedithioate HL3, methyl-3-hydroxy-3-(9-anthracyl)-2-propenedithioate HL4 and methyl-3-hydroxy-3-(*p*-fluorophenyl)-2-propenedithioate HL5 were synthesized according to the procedure as reported earlier [22,23]. To a solution of NaH (0.6 g, 25 mmol) dissolved in DMF: *n*-hexane mixture (4:1; 20 mL) was added gradually 4-acetylpyridine (1.21 g, 10.0 mmol) (for HL1), *p*-chloroacetophenone (1.54 g, 10.0 mmol) (for HL2), 2-acetylnaphthalene (1.7 g, 10.0 mmol) (for HL3), 9-acylanthracene (2.20 g, 10.0 mmol) (for HL4) and *p*-fluoroacetophenone (1.38 g, 10.0 mmol) (for HL5) in DMF (20 mL) separately. The reaction mixture was stirred for 1 h in an ice bath under N_2 atmosphere and a solution of dimethyltrithiocarbonate (TTC) (1.38 g, 10.0 mmol) was added slowly and



Scheme 2. Synthetic methodology for the potassium salts KL1–KL5 and their corresponding complexes **1–5**.

the mixture was further stirred for 10 h at room temperature. Excess NaH was neutralized by addition of 0.1 M HCl (50 mL), and the product was extracted with dichloromethane (3×50 mL), washed with brine solution and water, concentrated and dried over anhydrous Na_2SO_4 . The product thus obtained was purified by silica gel (100–200 mesh) chromatography using *n*-hexane as the eluent to collect crystalline yellow solids and characterized by IR and NMR spectroscopy (Ligand characterization data, in S3).

2.3. Synthesis of complexes (1–5)

For the synthesis of complexes, potassium salts of the ligands (KL1–KL5) were generated by stirring a 10 mL acetone solution of β -oxodithioesters HL1–HL5 (1 mmol) and solid K_2CO_3 (0.21 g, 1.5 mmol) for 4–5 h under reflux conditions. This was filtered off and the solution was dried on a vacuum evaporator to yield yellow to orange solids of the KL1–KL5.

To a stirred (10 mL) methanolic solution of KL1 (0.21 g, 1 mmol), KL2 (0.24 g, 1 mmol), KL3 (0.26 g, 1 mmol), KL4 (0.31 g, 1 mmol) or KL5 (0.22 g, 1 mmol) was slowly added a suspension of $\text{PhHg}(\text{CO}_2\text{CH}_3)$ (0.336 g, 1 mmol) in 10 mL methanol separately. Yellow precipitate was formed within a short while and the reaction mixture was further stirred for 3 h at room temperature (Scheme 2). The yellow solids thus formed were filtered off and washed with methanol followed by diethyl ether. The yellow crystals of complexes **1–5** were obtained by slow evaporation in dichloromethane solution within 2–3 weeks.

2.3.1 [PhHg(L1)] **1**: Yield: (0.38 g, 79%). M.pt. 172–175°C. Anal. Calcd for $\text{C}_{15}\text{H}_{13}\text{HgNOS}_2$ (487.97): C 36.92, H 2.69, N 2.87%. Found: C 36.72, H 2.80, N 3.05%. IR (KBr, cm^{-1}): 1592 ($\nu_{\text{C=O}}$), 1472 ($\nu_{\text{C=C}}$), 1059 ($\nu_{\text{C-S}}$). ^1H NMR (500 MHz, CDCl_3 , ppm): δ 2.65 (s, 3H, $-\text{SCH}_3$), 6.94 (1H, s, $-\text{CH}=\text{C}-$), 7.69–8.77 (m, 4H, $\text{C}_5\text{H}_4\text{N}$), 7.30–7.44 (m, 5H, Ar–H). $^{13}\text{C}\{^1\text{H}\}$ NMR (125 MHz, CDCl_3 , ppm): δ 19.01 ($-\text{SCH}_3$), 113.84 ($-\text{CH}=\text{C}-$), 121.25, 146.72, 150.80 ($\text{C}_5\text{H}_4\text{N}$), 129.16, 129.20, 136.57, 137.77 (Ar–C), 172.35 ($-\text{C=O}$), 185.01 ($=\text{C-S-}$).

UV-Vis. (CH_2Cl_2 , λ_{max} (nm), ε ($\text{M}^{-1} \text{ cm}^{-1}$)): 270 (2.86×10^4), 330 (1.28×10^4).

2.3.2 [PhHg(L2)] **2**: Yield: (0.42 g, 80%). M.pt. 158–161°C. Anal. Calcd for $\text{C}_{16}\text{H}_{13}\text{ClHgOS}_2$ (521.42): C 36.85, H 2.51%. Found: C 36.64, H 2.64%. IR (KBr, cm^{-1}): 1588 ($\nu_{\text{C=O}}$), 1476 ($\nu_{\text{C=C}}$), 1091 ($\nu_{\text{C-S}}$). ^1H NMR (500 MHz, CDCl_3 , ppm): δ 2.64 (s, 3H, $-\text{SCH}_3$), 6.97 (s, 1H, $-\text{CH}=\text{C}-$), 7.30–7.89 (m, 9H, Ar–H). $^{13}\text{C}\{^1\text{H}\}$ NMR (125 MHz, CDCl_3 , ppm): δ 19.23 ($-\text{SCH}_3$), 114.82 ($-\text{CH}=\text{C}-$), 129.21–138.85 (Ar–C), 168.88 ($-\text{C=O}$), 185.86 ($=\text{C-S-}$). UV-Vis. (CH_2Cl_2 , λ_{max} (nm), ε ($\text{M}^{-1} \text{ cm}^{-1}$)): 258 (1.03×10^4), 380 (2.77×10^4).

2.3.3 [PhHg(L3)] **3**: Yield: (0.44 g, 82%). M.pt. 140–143°C. Anal. Calcd for $\text{C}_{20}\text{H}_{16}\text{HgOS}_2$ (537.04): C 44.73, H 3.00%. Found: C 44.51, H 3.13%. IR (KBr, cm^{-1}): 1597 ($\nu_{\text{C=O}}$), 1475 ($\nu_{\text{C=C}}$), 1124 ($\nu_{\text{C-S}}$). ^1H NMR (500 MHz, CDCl_3 , ppm): δ 2.75 (s, 3H, $-\text{SCH}_3$), 7.39 (1H, s, $-\text{CH}=\text{C}-$), 7.49–8.50 (m, 12H, Ar–H). $^{13}\text{C}\{^1\text{H}\}$ NMR (125 MHz, CDCl_3 , ppm): δ 18.98 ($-\text{SCH}_3$), 115.34 ($-\text{CH}=\text{C}-$), 124.50–157.60 (Ar–C), 167.18 ($-\text{C=O}$), 186.85 ($=\text{C-S-}$). UV-Vis. (CH_2Cl_2 , λ_{max} (nm), ε ($\text{M}^{-1} \text{ cm}^{-1}$)): 245 (1.55×10^4), 394 (1.88×10^4).

2.3.4 [PhHg(L4)] **4**: Yield: (0.46 g, 78%). M.pt. 146–149°C. Anal. Calcd for $\text{C}_{24}\text{H}_{18}\text{HgOS}_2$ (587.09): C 49.10, H 3.09%. Found: C 48.87, H 3.22%. IR (KBr, cm^{-1}): 1590 ($\nu_{\text{C=O}}$), 1463 ($\nu_{\text{C=C}}$), 1133 ($\nu_{\text{C-S}}$). ^1H NMR (500 MHz, CDCl_3 , ppm): δ 2.34 (s, 3H, $-\text{SCH}_3$), 6.62 (1H, s, $-\text{CH}=\text{C}-$), 7.18–8.40 (m, 14H, Ar–H). $^{13}\text{C}\{^1\text{H}\}$ NMR (125 MHz, CDCl_3 , ppm): δ 19.01 ($-\text{SCH}_3$), 121.19 ($-\text{CH}=\text{C}-$), 125.39–137.65 (Ar–C), 167.82 ($-\text{C=O}$), 193.66 ($=\text{C-S-}$). UV-Vis. (CH_2Cl_2 , λ_{max} (nm), ε ($\text{M}^{-1} \text{ cm}^{-1}$)): 255 (1.154×10^5), 350 (0.83×10^4), 370 (1.09×10^4), 386 (1.13×10^4).

2.3.5 [PhHg(L5)] **5**: Yield: (0.42 g, 84%). M.pt. 120–123°C. Anal. Calcd for $\text{C}_{16}\text{H}_{13}\text{FHgOS}_2$ (504.97): C 38.06, H 2.59%. Found: C 37.82, H 2.71%. IR (KBr, cm^{-1}): 1595 ($\nu_{\text{C=O}}$), 1477 ($\nu_{\text{C=C}}$), 1053 ($\nu_{\text{C-S}}$). ^1H NMR (500 MHz, CDCl_3 , ppm): δ 2.61 (s, 3H, $-\text{SCH}_3$), 6.95 (1H, s, $-\text{CH}=\text{C}-$), 7.10–7.95 (m, 9H, Ar–H). $^{13}\text{C}\{^1\text{H}\}$ NMR (125 MHz, CDCl_3 , ppm): δ 18.97 ($-\text{SCH}_3$), 114.65 ($-\text{CH}=\text{C}-$), 115.60–166.29 (Ar–C), 167.69 ($-\text{C=O}$), 185.41 ($=\text{C-S-}$). UV-Vis. (CH_2Cl_2 , λ_{max} (nm), ε ($\text{M}^{-1} \text{ cm}^{-1}$)): 256 (1.61×10^4), 352 (2.41×10^4).

2.4. X-ray crystal structure determination

Single crystals of **1–5** were obtained by slow evaporation of solutions of the compound in CH_2Cl_2 . Single crystal X-ray diffraction data for complexes **1–4** were collected on an Oxford Xcalibur CCD diffractometer at 150 K using Mo $\text{K}\alpha$ radiation and **5** on a Bruker D8 Quest SCM X-ray diffractometer at 100 K. Data analysis was carried out using the CrysAlis program [30]. All structures were solved using direct methods with the SHELXS-97 [31] and refined on F^2 by full matrix least-squares method using SHELXL2016-6 [32]. The non-hydrogen atoms were refined with anisotropic thermal parameters. The hydrogen atoms bonded to carbon were included in geometric positions and given thermal parameters equivalent to 1.2 times those of the atom to which they were attached. The $-\text{SMe}$ group in complex **3** was disordered over two positions. Crystals of both complexes **2** and **3** were twinned. Diagrams for the complexes were prepared using OLEX2 [33] and Mercury [34] software. Crystal data for **1–5** were deposited at the Cambridge Crystallographic Data Centre with reference numbers CCDC 1532701, 1570469, 1570468, 2004456 and 2004457.

2.5. Theoretical calculations

Single point calculations were carried out using the Gaussian 03 program [35]. Structures were carried out using the B3LYP density functional together with basis sets LANL2DZ for Hg, 6-31+G* for S, N and O and 6-31G for C and H. Starting models were taken from the crystal structures but with hydrogen atoms given normalised positions via GaussView [36].

3. Results and discussion

3.1. Synthesis and characterization

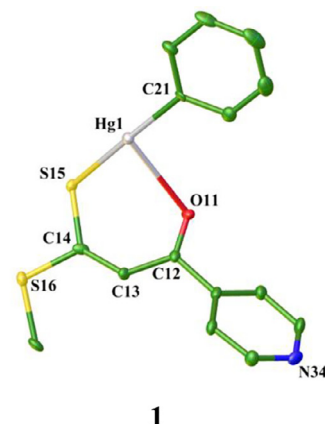
Treatment of a methanolic solution of PhHg(OAc) with the potassium salts of the β -oxodithioester ligands, KL1–KL5 in an equimolar ratio, resulted in the formation of air- and moisture stable light yellow solids of PhHg(II) β -oxodithioester complexes **1–5** in good yields (Scheme 2). They are insoluble in common organic solvents such as ethanol, methanol, acetone, acetonitrile, benzene but are soluble in dichloromethane, DMF and DMSO. Complexes were characterized by elemental analysis, spectroscopy (IR, UV-Vis., ^1H and $^{13}\text{C}\{^1\text{H}\}$) and their solid state structures have been determined by single crystal X-ray diffraction. Homogeneity of the bulk samples of **1–5** was confirmed by comparing the observed PXRD patterns with the respective simulated powder patterns observed from the single crystal data. The experimental and simulated PXRD patterns are well in agreement indicating the phase purity of the bulk samples (Fig. S1). Complexes **1–5** exhibit bright green luminescence characteristics in solution and solid phases. The semiconducting behaviour of the complexes was investigated by pressed pellet electrical conductivity measurements.

3.2. Spectroscopic Studies

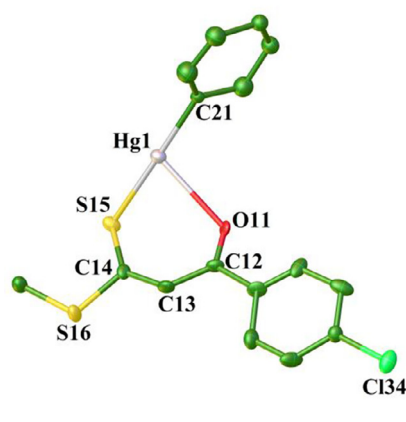
In the IR spectra, the characteristic $\nu_{\text{C}-\text{OH}}$, $\nu_{\text{C}=\text{S}}$ and $\nu_{\text{C}=\text{C}}$ vibrations of uncoordinated β -oxodithioester ligands appear in the regions 1060–1165, 1217–1245 and 1579–1601 cm^{-1} respectively. In complexes **1–5** these vibrations occur at 1588–1597, 1053–1133 and 1463–1477 cm^{-1} respectively. A perceptible decrease in the $\nu_{\text{C}-\text{S}}$ frequency in the complexes as compared to the ligands indicates the coordination via S-atom of the $-\text{SCSMe}$ group of the β -oxodithioester ligands.

In the ^1H NMR spectra, the ligands HL1–HL5 show the $-\text{OH}$ proton resonances in the δ 14.78–15.37 ppm range which are ab-

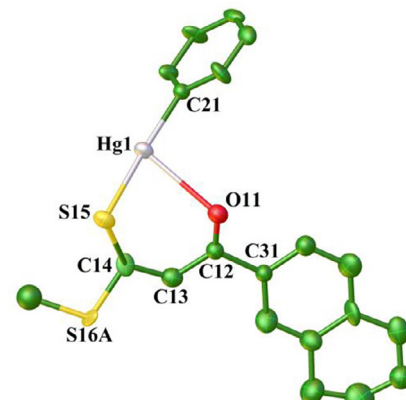
sent in the complexes **1–5**. The signal for vinylic proton in the free ligands (δ 6.83–7.10 ppm) and their corresponding complexes (δ 6.62–7.39 ppm) remains almost unchanged. The position of the methyl protons of $-\text{SCH}_3$ in the complexes revealed no noticeable shift and appeared in the range δ 2.34–2.75 ppm. In the $^{13}\text{C}\{^1\text{H}\}$ NMR spectra, the resonances for the C–OH carbon are observed at



1



2



3

Fig. 1. ORTEP diagrams of the complexes **1–5** with displacement ellipsoids at 30% probability. H atoms have been omitted for clarity.

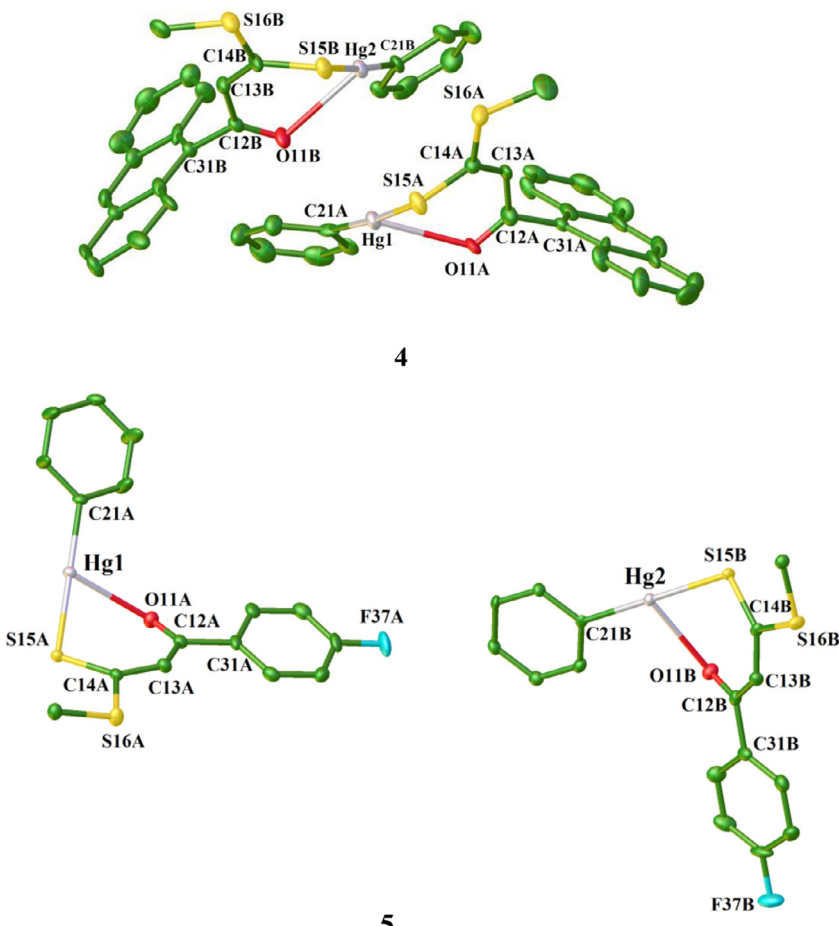


Fig. 1. Continued

δ 165.30–170.18 ppm and δ 167.18–172.35 ppm in the uncoordinated ligands and their complexes, respectively. The vinylic carbon of the ligands at δ 107.53–115.17 ppm is slightly downfield shifted at δ 113.84–121.19 ppm in the complexes. The $-\text{C}=\text{S}$ carbon at δ 216.62–219.27 ppm in the free ligands shows an upfield shift and is observed at δ 185.01–193.66 ppm in the complexes indicating metal–sulfur bonding. This indicates that the keto form of the β -oxodithioester ligand is stabilized in these complexes [20] (crystal structures *vide infra*).

3.3. Crystal structures

Single crystals of **1–5** were grown by slow evaporation of a CH_2Cl_2 solution. Crystallographic data and structure refinement parameters for all crystals are presented in Table 1 and the selected bond lengths and bond angles are listed in Table 2. ORTEP diagrams of the complexes with displacement ellipsoids at 30% probability are shown in Fig. 1. In **1**, **2** and **3**, the asymmetric unit contains a single discrete molecule whereas complexes **4** and **5** contain two independent molecules.

In **1–5**, two-coordinate geometry about the Hg atom is defined [37] by the *ipso*-C of the phenyl ring at 2.036(18)–2.084(13) Å and S15 of the β -oxodithioester at 2.350(5)–2.386(5) Å with the C21–Hg1–S15 angles of 174.2(4)–178.5(3) $^\circ$ indicating small but significant deviations from linearity. The Hg1...O11 distances of 2.622(10)–2.813(6) Å in **1–5** are somewhat longer but significantly less than the sum of van der Waals radii [38] of 3.23 Å. This weaker bond establishes a distorted T-shaped structure about the Hg atom with C21–Hg1–O11, S15–Hg1–O11 and C21–Hg1–S15 angles,

respectively, at 102.0(3), 75.1(1) and 174.8(2) $^\circ$ for **1**, 101.7(10), 79.2(4) and 178.2(11) $^\circ$ for **2**, 99.5(8), 77.8(6) and 177.2(9) $^\circ$ for **3**, 106.4(5), 79.1(3) and 174.2(4) for **4A**; 105.2(5), 80.5(3) and 174.3(4) $^\circ$ for **4B**, 101.2(2), 79.7(1) and 178.5(2) for **5A**; 99.9(2), 79.4(1) and 178.1(2) $^\circ$ for **5B**.

In **1**, the distant pyridyl N in the 4-position of the β -oxodithioester ligand L1 of a neighbouring molecule is oriented to Hg atom forming intermolecular Hg...N34\$2 contacts [2, 4b–e] ($\$2 = -1+x, \frac{1}{2}-y, -1/2+z$) at a somewhat longer distance of 2.938(7) Å which is well within the range of intermolecular Hg–N contacts [39]. Simultaneously the S15\$1 atom in a different adjacent ligand molecule ($\$1 = x, 1/2-y, -1/2+z$) is attached to Hg atom forming intermolecular Hg...S contacts at 3.230(2) Å leading to a 2-D net-like polymeric structure (Fig. 2). By comparison in the reported [20] analogous PhHg(II) β -oxodithioester complex the pyridyl N in the 3-position forms 1-D coordination polymeric structure. The sulfur atom of the $-\text{SMe}$ group is not involved in the formation of Hg...S contacts due to its poor electron donating capability. Considering the metal-assisted intra- and intermolecular secondary bonding interactions, the Hg atom can be considered to be five-co-ordinate (Fig. 2b) with a geometry intermediate between square pyramidal and trigonal bipyramidal with a τ value of 0.497 [40]. The observed bond angles are N34\$2–Hg1–O11 145.0(2) $^\circ$, O11–Hg1–S15\$1 127.7(1) $^\circ$, S15\$1–Hg1–N34\$2 76.9(1) $^\circ$ and S15\$1–Hg1–C21 92.7(1) $^\circ$. It is worth noting that in this complex the carbonyl oxygen is bonded to Hg atom at 2.813(6) Å, a distance significantly longer than those found in **2–5** but still significantly smaller than the sum of van der Waals radii of 3.23 Å [30]. This bond lengthening can presumably be attributed to the

Table 1
Crystallographic data and refinement parameters for complexes **1–5**.

Compound	1	2	3	4	5
Chemical formula	C ₁₅ H ₁₃ HgNOS ₂	C ₁₆ H ₁₃ ClHgOS ₂	C ₂₀ H ₁₆ HgOS ₂	C ₂₄ H ₁₈ HgOS ₂	C ₁₆ H ₁₃ FHgOS ₂
Formula weight	487.97	521.42	537.04	587.09	504.97
Crystal system	monoclinic	monoclinic	monoclinic	monoclinic	monoclinic
Space group	P2 ₁ /c	P2 ₁	P2 ₁	P2 ₁ /c	P2 ₁ /c
a (Å)	10.1483(7)	11.5285(8)	12.6105(19)	8.2006(6)	25.8140(13)
b (Å)	21.8960(13)	5.3034(3)	5.4072(6)	17.493(2)	5.2441(3)
c (Å)	7.2581(4)	13.1702(9)	12.9648(18)	28.7380(18)	23.1032(11)
β(°)	110.451(7)	95.889(7)	96.201(14)	90.012(6)	101.356(2)
V (Å ³)	1511.15(17)	800.98(9)	878.9(2)	4122.6(6)	3066.3(3)
Z	4	2	2	8	8
ρ _{calc} (g cm ⁻³)	2.145	2.162	2.029	1.892	2.188
T (K)	150(2)	150(2)	150(2)	150(2)	100(2)
μ(Mo Kα) (mm ⁻¹)	10.455	10.029	8.997	7.681	10.316
F(000)	920	492	512	2256	1904
Reflections collected	9867	5517	4154	20593	46736
Independent reflns	4210	2286	1931	11166	7558
Reflections with I > 2σ(I)	3173	2016	1504	5931	6291
Final indices [I > 2σ(I)] R ₁ ^a , wR ₂ ^b	0.0535, 0.0988	0.0589, 0.1583	0.0795, 0.1797	0.0829, 0.1678	0.0331, 0.0837
R ₁ [a], wR ₂ [b][all data]	0.0767, 0.1080	0.0675, 0.1647	0.1018, 0.1919	0.1629, 0.2024	0.0469, 0.0932
GOF	1.005	1.019	1.058	0.935	1.070
Max., min. residual electron density (e/ Å ³)	3.303, -2.389	3.444, -1.345	3.288, -1.855	2.661, -3.297	1.759, -1.549

^a R₁ = Σ ||F₀| - |F_c|| / Σ|F₀|.^b R₂ = { [Σw(F_o² - F_c²) / Σw(F_o²)²] }^{1/2}, w = 1/[σ²(F_o²) + (xP)²], where P = (F_o² + 2F_c²)/3.

Table 2
Bond lengths and bond angles in complexes **1–5**.

Bond Lengths (Å)	1	2	3	4A	4B	5A	5B
Hg1-O11	2.813(6)	2.674(12)	2.73(2)	2.688(10)	2.622(10)	2.645(4)	2.640(4)
Hg1-S15	2.377(2)	2.386(5)	2.380(7)	2.350(5)	2.371(5)	2.3802(14)	2.3752(14)
Hg1-C21	2.059(7)	2.077(15)	2.084(13)	2.036(18)	2.060(18)	2.071(6)	2.081(5)
Hg1-S15\$1	3.230(2)	3.326(11)	3.285(17)	n/a*	n/a*	3.296(1)	3.3236(14)
O11-C12	1.241(9)	1.23(2)	1.19(3)	1.211(18)	1.273(18)	1.248(7)	1.242(7)
C12-C13	1.426(11)	1.46(3)	1.43(4)	1.43(2)	1.438(18)	1.425(8)	1.430(8)
C13-C14	1.359(10)	1.41(3)	1.43(4)	1.34(2)	1.37(2)	1.365(8)	1.367(8)
C14-S15	1.746(8)	1.73(2)	1.70(3)	1.737(15)	1.734(15)	1.732(6)	1.737(5)
C14-S16	1.750(9)	1.77(2)	1.80(2)	1.754(14)	1.743(16)	1.760(6)	1.762(6)

Bond Angles (°)	1	2	3	4A	4B	5A	5B
C21-Hg1-S15	174.75(19)	178.2(11)	177.2(9)	174.2(4)	174.3(4)	178.49(16)	178.06(13)
C21-Hg1-O11	102.0(3)	101.7(10)	99.5(8)	106.4(5)	105.2(5)	101.16(18)	99.90(17)
O11-Hg1-S15	75.07(13)	79.2(4)	77.6(6)	79.1(3)	80.5(3)	79.67(10)	79.43(10)
Hg1-O11-C12	110.3(5)	119.4(16)	117.9(18)	120.3(10)	118.6(8)	119.0(4)	119.2(4)
O11-C12-C13	125.8(7)	126(2)	127(3)	124.0(17)	125.9(15)	124.0(6)	123.8(6)
C12-C13-C14	128.4(7)	125.4(19)	124(3)	129.6(16)	128.7(16)	129.2(6)	128.9(5)
C13-C14-S15	129.4(7)	133.3(17)	134(2)	129.9(11)	129.8(12)	131.6(5)	131.5(5)
Hg1-S15-C14	106.9(3)	105.0(6)	103.8(9)	103.8(6)	106.0(7)	105.60(19)	106.0(2)
S15-C14-S16	107.9(4)	115.9(11)	120.4(15)	105.8(8)	108.9(9)	116.6(3)	116.3(3)

Symmetry element \$1 In **1** -1+x, ½-y, -½+z; in **2** 1-x, -1/2+y, 2-z; in **3** 1-x, y+1/2, 1-z; in **5A** 1-x, y+1/2, ½-z; in **5B**

2-x, y+1/2, 3/2-z

* no sulfur atom in the equatorial plane

orientation of the pyridyl group in the polymeric network which forces the carbonyl oxygen slightly away from the metal. In order to test the importance of the two intermolecular interactions described above, single point calculations were carried out on two molecules so associated and E(dimer) – 2*E(monomer) showed favorable interactions. That calculated involving the N34\$2 interaction (coordinates x, y, z and -1+x, ½-y, -1/2+z) gave an energy difference of 4.50 kcal mol⁻¹ and that for the S15\$1 interaction (coordinates x, y, z and x, 1/2-y, -1/2+z) 3.57 kcal mol⁻¹.

Likewise in complexes **2** and **3** derived from the *p*-chlorophenyl and 2-naphthyl β-oxodithioester ligand L2 and L3 respectively, the Hg atom is three coordinate T-shaped being bonded to the *ipso*-carbon C21 of a phenyl ring, S15 and O11 atoms of β-

oxodithioester ligand L2 and L3 at 2.077(15), 2.076(9), 2.084(13) Å; and 2.674(12), 2.653(7), 2.726(12) Å respectively. Also the metal centre is weakly bonded to S15\$1 atoms in adjacent molecules at 3.326(11) Å, \$1 = 1-x, y-1/2, 2-z in **2**; and 3.285(17) Å \$1 = 1-x, ½+y, 1-z in **3** resulting in the formation of 1-D linear zig-zag polymeric chain along a screw axis (*Figs. 3* and *4*). The significance of this weak interaction between the metal and S15\$1 can be evaluated by the fact that it is present in all three structures as well as in complex **5** despite the structures having very different unit cells (*vide supra*). Therefore a rare distorted square planar coordination environment particularly with a d¹⁰ metal centre is established in these complexes. In **2** the four donor atoms show an r.m.s. deviation of 0.169 Å with the metal atom 0.134(10) Å from the plane.

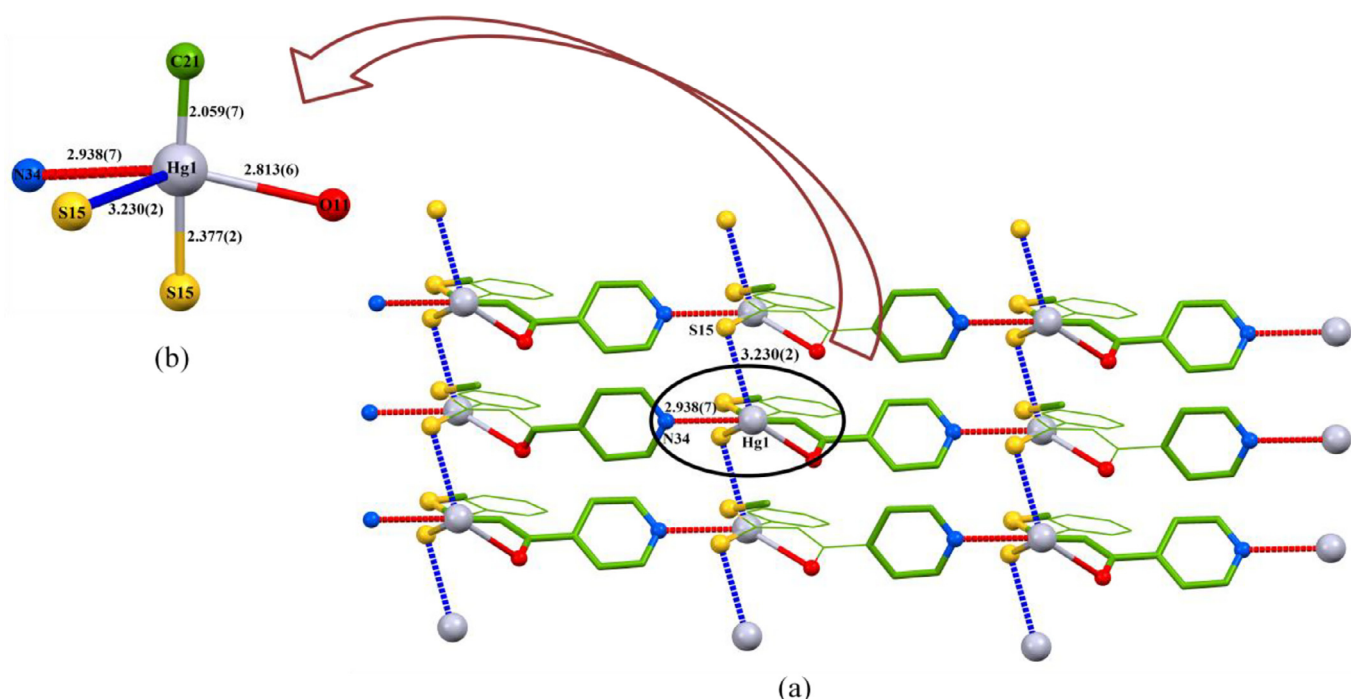


Fig. 2. (a) 2-D polymeric chain motif in **1** via intermolecular Hg-S15\$1 (3.230(2) Å) and Hg-N34\$2 (2.938(7) Å) bonding interactions. (b) The distorted five-coordinate environment of the metal centre in **1**. Distances are reported in Å.

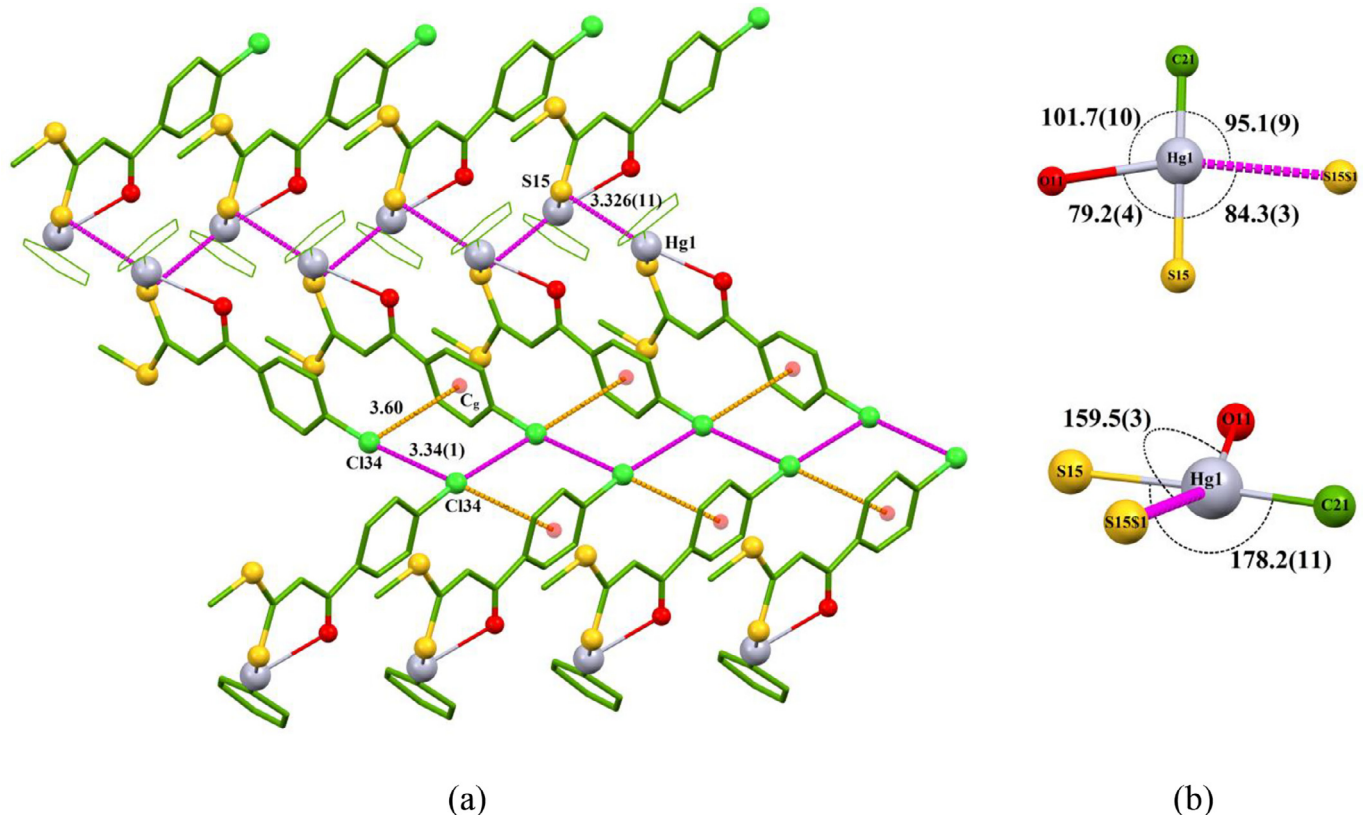


Fig. 3. (a) 1-D polymeric chain view of **2** showing intermolecular Hg...S, Cl...Cl and Cl...π bonding interactions. (b) Bond angles about mercury atom showing distorted planar coordination. Distances are reported in Å and angles in degree (°).

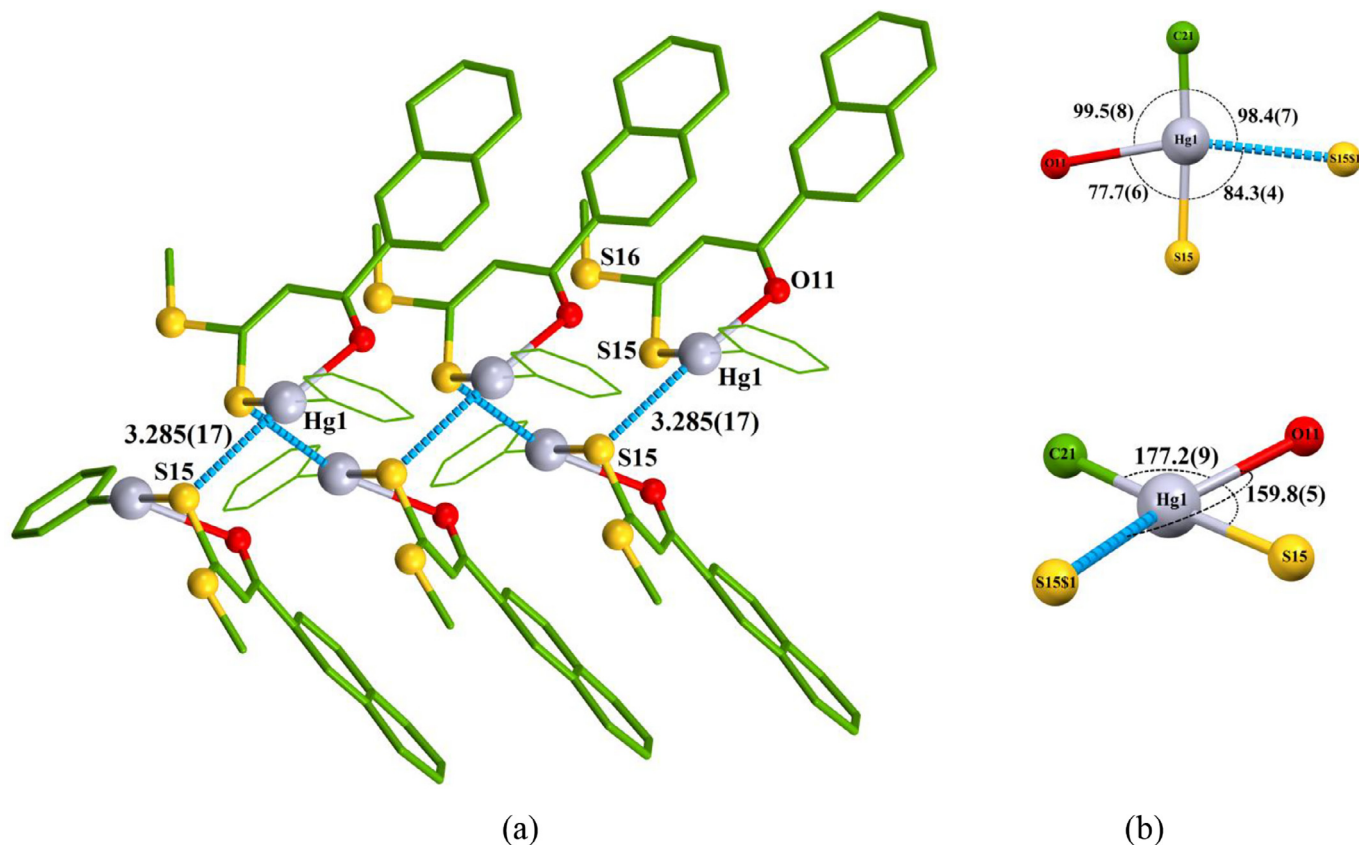


Fig. 4. 1-D polymeric chain view of **3** showing intermolecular $\text{Hg}\cdots\text{S}$ bonding interactions. (b) Bond angles about mercury atom showing distorted square planar coordination. Distances are reported in Å and angles in degree (°).

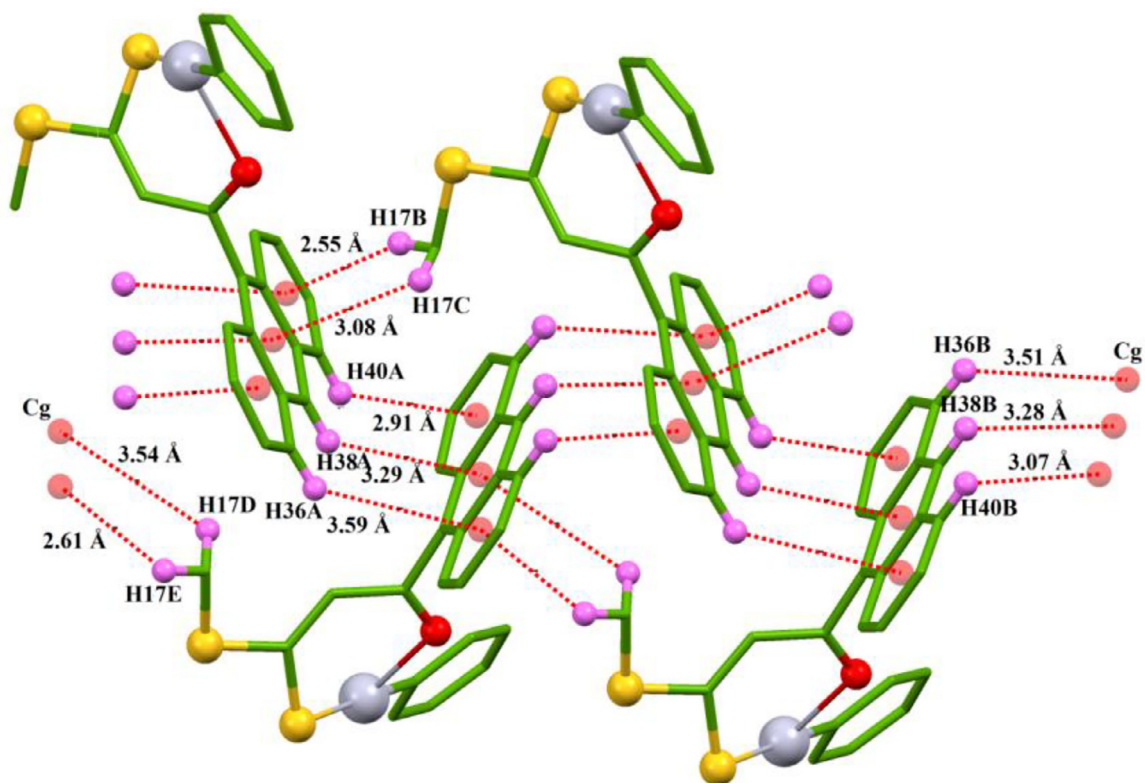


Fig. 5. 1-D polymeric chain motif network in **4** formed through $\text{C}-\text{H}\cdots\pi$ interactions. Hydrogen atoms not involved in interactions are omitted.

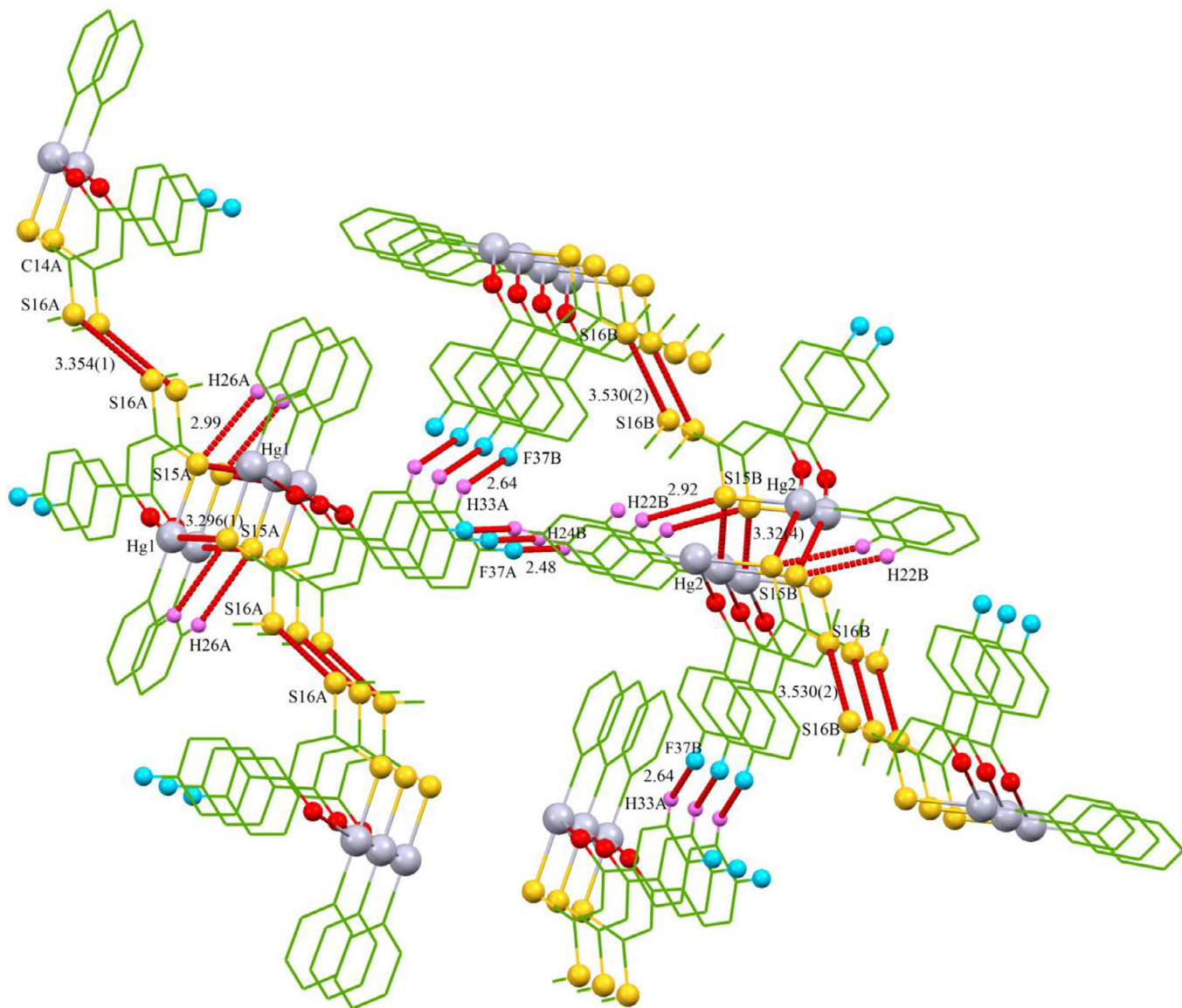


Fig. 6. Supramolecular structure of **5** sustained by weak intermolecular $\text{Hg}\cdots\text{S}$, $\text{S}\cdots\text{S}$, $\text{S}\cdots\text{H}$ and non-covalent $\text{C}-\text{H}\cdots\text{F}$ interactions. Hydrogen atoms not involved in interactions are omitted. Distances are reported in Å.

Equivalent value is 0.116, 0.122(10) Å in **3**. In the crystal structure of **2**, the supramolecular structure is stabilized by a chain of weak $\text{Cl}34\cdots\text{Cl}34\1 ($\$1 = -x, \frac{1}{2}+y, 1-z$ and $-x, -1/2+y, 1-z$) along the y axis at (3.34(1) Å) and $\text{Cl}34\cdots\pi\$2$ ($\$2 = x, -1+y, z$) (3.60 Å) interactions (Fig. 3).

Unlike **1–3**, the crystal structures of **4** and **5** contain two independent molecules in the asymmetric unit (Fig. 1). In **4**, there are only slight variations between the dimensions in the A and B molecules, thus the $\text{Hg}1\cdots\text{S}15\text{A}$, $\text{Hg}2\cdots\text{S}15\text{B}$ and $\text{Hg}1\cdots\text{O}11\text{A}$, $\text{Hg}2\cdots\text{O}11\text{B}$ distances are 2.350(5) Å, 2.371(5) Å and 2.688(10) Å, 2.622(10) Å respectively. However the structure is unique, very different from those found in **1**, **2**, **3** and **5**. The steric bulk of anthracene group has prevented any prominent weaker bonding interactions to organize the supramolecular networks in **4** and so there is no polymer formation. There are intermolecular weak $\text{Hg}\cdots\text{S}$ contacts $\text{Hg}1\cdots\text{S}15\text{B}$ ($1+x,y,z$) at 3.529(7) Å and $\text{Hg}2\cdots\text{S}16\text{A}$ at 3.419(7) Å but these are longer than the shortest intermolecular $\text{Hg}\cdots\text{S}$ contacts found in **2** and **3** and also in very different orientations as they are not positioned in the equatorial plane. And it will be noted that these interactions involve A molecules mixed

together with B molecules. The metal atoms can therefore best be considered as three-coordinate.

Many $\text{C}-\text{H}\cdots\pi$ interactions are found in **4** (Fig. 5) involving the anthracene rings with distances (d) of 3.51 Å involving $\text{H}36\text{B}$ and centre of gravity (Cg) of ring containing atoms $\text{C}39\text{A}\cdots\text{C}44\text{A}$ inclusive, d 3.28 Å involving $\text{H}38\text{B}$ and Cg $\text{C}31\text{A}\cdots\text{C}44\text{A}$, d 3.07 Å involving $\text{H}40\text{B}$ and Cg $\text{C}32\text{A}\cdots\text{C}37\text{A}$, d 3.59 Å involving $\text{H}36\text{A}$ and Cg $\text{C}39\text{B}\cdots\text{C}44\text{B}$, d 3.29 Å involving $\text{H}38\text{A}$ and Cg $\text{C}31\text{B}\cdots\text{C}44\text{B}$, d 2.91 Å involving $\text{H}40\text{A}$ and Cg $\text{C}32\text{B}\cdots\text{C}37\text{B}$, d 2.55 Å involving $\text{H}17\text{B}$ and Cg $\text{C}39\text{A}\cdots\text{C}44\text{A}$, d 3.08 Å involving $\text{H}17\text{C}$ and Cg $\text{C}31\text{A}\cdots\text{C}44\text{A}$, d 3.54 Å involving $\text{H}17\text{D}$ and Cg $\text{C}31\text{B}\cdots\text{C}44\text{B}$ and d 2.61 Å involving $\text{H}17\text{E}$ and Cg $\text{C}32\text{B}\cdots\text{C}37\text{B}$.

By contrast in **5** there are shorter $\text{Hg}\cdots\text{S}$ contacts comparable to those found in **2** and **3** which form similar but distinct independent polymers for molecules A and B both along a screw axis. Distances are $\text{Hg}1\cdots\text{S}15\text{A} \1 ($\$1 = 1-x, \frac{1}{2}+y, \frac{1}{2}-z$) at 3.296(1) Å and $\text{Hg}2\cdots\text{S}15\text{B} \1 ($\$1 = 2-x, \frac{1}{2}+y, 3/2-z$) at 3.324(1) Å. Similar to those structures, the r.m.s. deviations from the square planes are 0.153 and 0.138 Å with the metal atoms 0.125(2), 0.172(2) Å from the planes in A and B respectively.

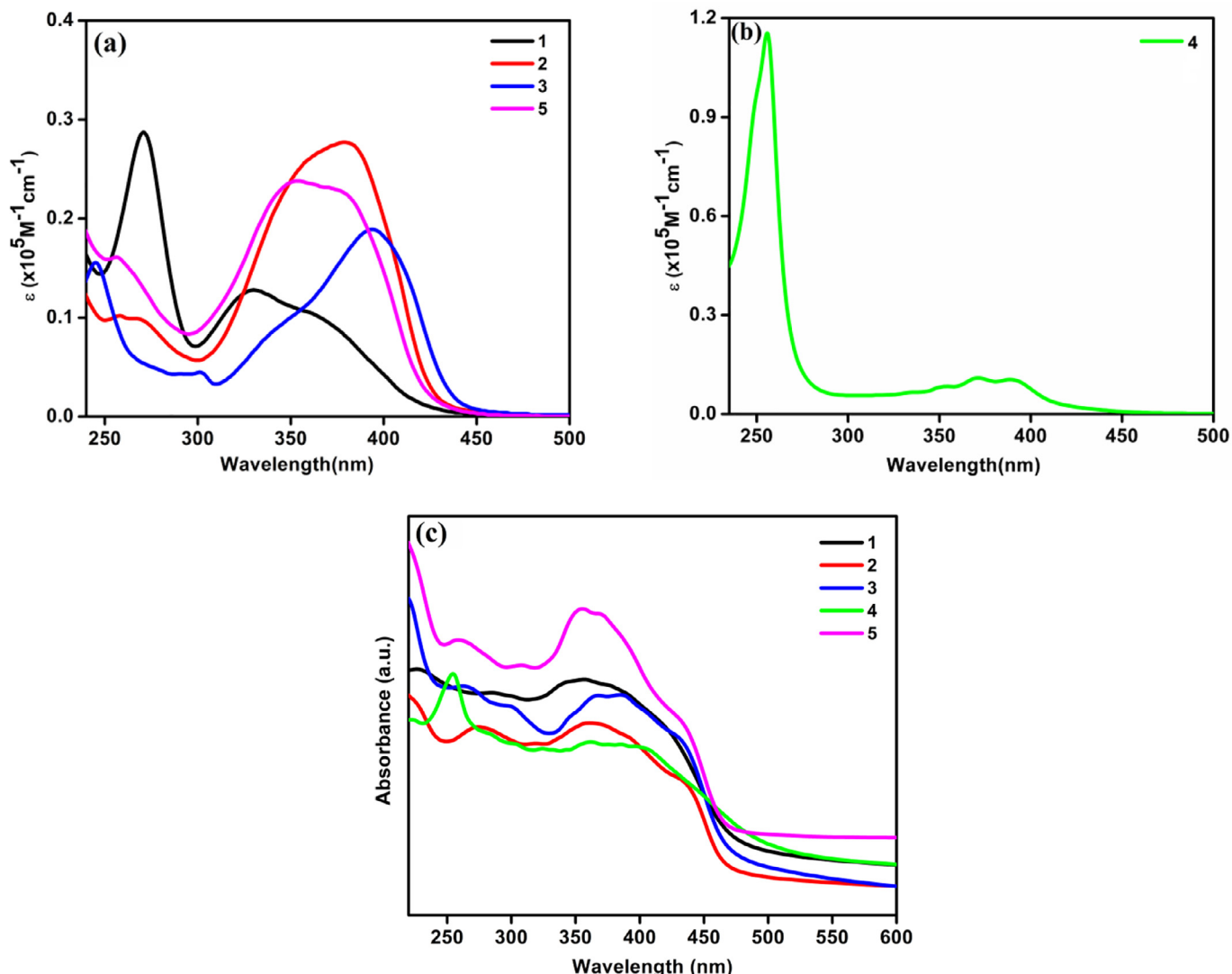


Fig. 7. (a) Electronic absorption spectra of complexes **1–3**, **5** (b) and complex **4** in CH₂Cl₂ solution and (c) solid state absorption spectra of **1–5** in Nujol mull.

The smaller *p*-fluorophenyl substituent on the β -oxodithioester backbone allowed prominent S...S interactions, namely S16A...S16A (1-x, 4-y, 1-z) of 3.354(1) Å and S16B...S16B (2-x, 1-y, 2-z) 3.530(2) Å, which connect the polymers formed along the screw axes described above via centres of symmetry to form two dimensional separate A and B polymers as shown in Fig 6. Additional C-H...S and C-H...F interactions at 2.99 Å, and 2.64 Å help to stabilize the supramolecular architecture. Among the structures other than **5** the shortest S...S distances are >=3.95 Å.

There are no significant Hg...Hg intermolecular distances in the five structures with the shortest distance of 4.108(1) Å significantly higher than the sum of van der Waals radii of 3.46 Å [38]. The crystal structures of **1**, **2** and **4** are also stabilized by weak C-H...S interactions. (Fig. S2)

The C12–O11 carbonyl bond lengths in the range 1.19(3)–1.273(18) Å in **1–5** are consistent with the partial double bonds. The C13–C14 bond lengths for **1–5** in the range 1.34(2)–1.44(4) Å show distinct double bond character. The C14–S15 distances of 1.70(3)–1.746(8) Å and the slightly longer C14–S16 distances of 1.743(16)–1.80(2) Å are in the range for the C–S single bond lengths. Thus some delocalization of electron density is observed over the six-membered chelate ring comprising of O11, C12, C13, C14, S15 and Hg1 atoms in these complexes (Fig. 1).

3.4. Optical properties

Absorption and Emission Spectra. The UV-Vis. absorption spectra of **1–5** in CH₂Cl₂ and solid as Nujol mull are presented in Fig. 7. In solution the absorption bands near 250–270 nm ($\epsilon = 1.01\text{--}11.54 \times 10^4 \text{ M}^{-1} \text{ cm}^{-1}$) and 350–400 nm ($\epsilon = 1.09\text{--}2.80 \times 10^4 \text{ M}^{-1} \text{ cm}^{-1}$) are mostly ligand centered and are assigned to intraligand charge transfer (ILCT) and slightly metal perturbed ILCT transitions respectively [3,5b–d] (Fig 7a, b). In solid as Nujol mull, they exhibit absorption bands near 250–280 nm and 340–440 nm (Fig. 7c); the features of the spectra in two media are almost similar apart from the differences in intensity of the absorptions and slight variations in their positions. This reveals that the structures of the complexes are virtually persistent in solution.

All the complexes displayed bright green luminescent emissions in solution and solid phases when irradiated in the UV-Vis. light. Upon excitation at 260 nm in CH₂Cl₂ solution, **1–3** and **5** display an unstructured medium broad emission bands near $\lambda_{\text{emis}}^{\text{max}}$ 330–420 nm with a Stokes shift of 100–140 nm (Fig. 8a) arising from the ILCT state. When excited at 350–360 nm, they show an unstructured broad emission bands at around $\lambda_{\text{emis}}^{\text{max}}$ 400 nm, with a relatively smaller Stokes shift of 50 nm (Fig. 8b). Interestingly complex **4** upon excitation at 260, 350, 370 and 386 nm ex-

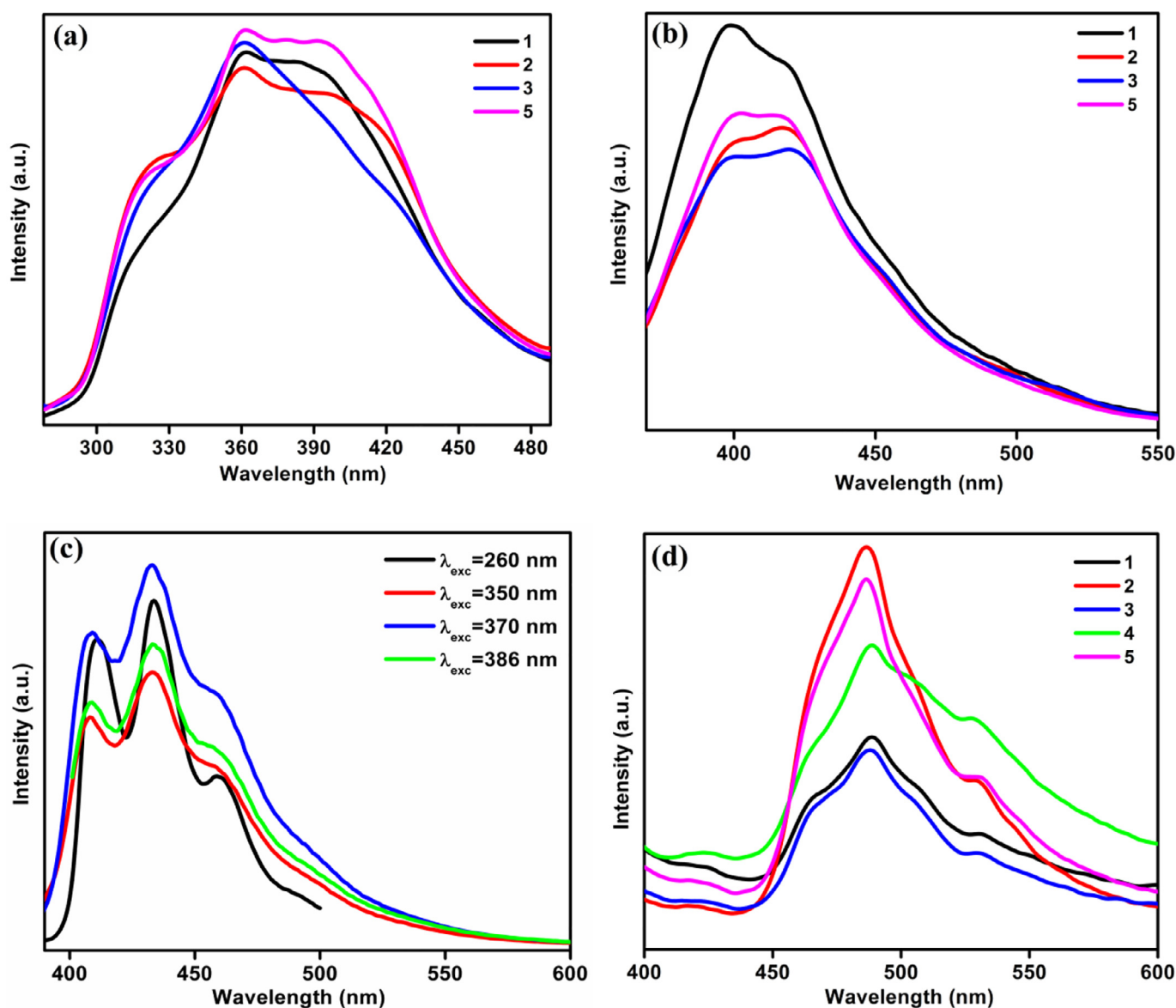


Fig. 8. Emission spectra of complexes **1–3, 5** at (a) $\lambda_{\text{ex}} = 260 \text{ nm}$; (b) $\lambda_{\text{ex}} = 350 \text{ nm}$, (c) and complex **4** at $\lambda_{\text{ex}} = 260 \text{ nm}, 350 \text{ nm}, 370 \text{ nm}, 386 \text{ nm}$ in CH_2Cl_2 solution (d) Solid phase emission spectra of **1–5** at room temperature, $\lambda_{\text{em}}^{\text{max}}$ at 390 nm.

hibits structured emission bands at 410, 430 and 460 nm (Fig. 8c) in solution characteristic of the anthracene group, obeying *Kasha's rule*; [41,42] the red shifted emissions in this compound may be attributed to enhanced delocalization provided by the anthracene group on the β -oxodithioester ligand L4. Upon excitation at 350 nm in the solid, **1–5** exhibit perceptible red shifted strong emission band at $\sim 500 \text{ nm}$ accompanied with a shoulder at 530 nm in comparison to their solution spectra (Fig. 8d). The prominent luminescent properties of all the complexes may be attributed to their almost identical luminescence chromophores as well as to the supramolecular architectures sustained via various metal assisted Hg...N, Hg...S and other weaker Cl...Cl, C-H...F and S...S intermolecular interactions in the solid state.

3.5. Pressed pellet conductivity

The temperature dependence of the pressed pellet electrical conductivities of the powdered complexes have been measured by conventional two-probe technique using a Keithley 236 electrometer in the temperature range 303–373 K (Fig. 9). The pel-

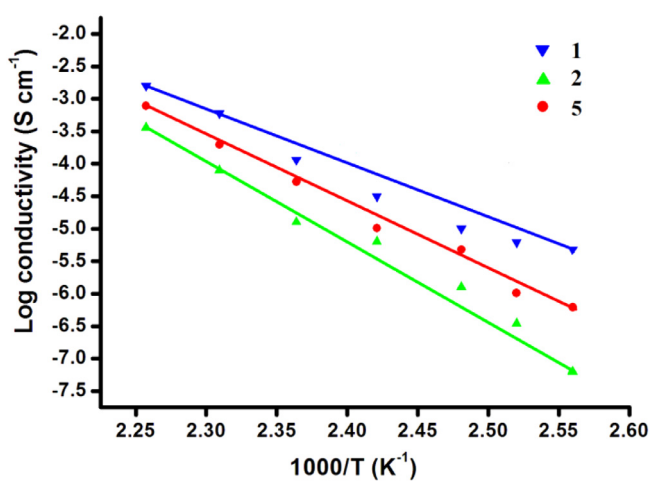


Fig. 9. Temperature dependent pressed pellet conductivity plots for complexes **1, 2** and **5**.

lets were made at a pressure of 2.0×10^5 kN m $^{-2}$ with tablet size 13 mm in diameter and 0.5 mm thickness and contacts on the pellet surfaces were made using silver paint. Complexes **1**, **2** and **5** with σ_{rt} values in the 10^{-3} - 10^{-6} S cm $^{-1}$ range are weakly conducting. Their lower conductivities may be attributed to the lack of S...S intermolecular contacts in the solid state (*vide supra* in the crystal structures) which is an important prerequisite for their higher conductivities [14]. They show behaviour of semiconductors in the measured temperature range of 303–373 K with Ea = 0.14–0.64 eV as their conductivities correlate with change in temperature.

4. Conclusions

Five new PhHg(II) complexes with functionalized β -oxodithioester ligands have been synthesized and well characterized. Their crystal structures revealed a linear geometry about the Hg atom, bound by the S15 atom of the β -oxodithioester ligand and C21 atom of the aromatic ring, the O atom of the ligand is weakly attached to the metal centre. In complex **1** the Hg atom is also weakly bonded to pyridyl N on 4-position on the β -oxodithioester in an adjacent molecule. Simultaneously the S atom on a different adjacent molecule is also attached to Hg atom forming a 2-D net-like polymeric structure. In these complexes varied supramolecular structures are sustained via Hg...N, Hg...S, C—H... π , Cl...Cl, Cl... π , S...S, C—H...S and C—H...F secondary interactions. All the complexes show bright green luminescent emissions in solution and solid phases. The stronger luminescent characteristics of **4** are attributed to the presence of higher conjugation in anthracene moieties on the dithioester unit. Temperature dependent pressed pellet conductivity measurements indicate semiconducting behaviour of the complexes. This study demonstrates that the electronic and steric properties of the substituents on the β -oxodithioester ligands backbone may substantially influence the solid state structures, bonding interactions, formation of supramolecular architectures as well as luminescent and conducting properties of the organomercury dithioester complexes and their possible applications as functional materials.

Declaration of Competing Interest

The authors declare that they have no known competing financial interests or personal relationships that could have appeared to influence the work reported in this paper.

Acknowledgements

NS and KK gratefully acknowledge financial support from the University Grants Commission (UGC), New Delhi for the award of BSR Faculty Fellow (ref No. F. 18-1/2011(BSR) 30 Dec 2016) and CSIR-SRF fellowship respectively. We are also thankful to the Department of Chemistry, Institute of Science, Banaras Hindu University, UGC CAS-II for infrastructural and instrumentation facilities. M.G.B. Drew acknowledges EPSRC (UK) and the University of Reading for funds for the X-Calibur system.

References

- [1] (a) G. Henkel, B. Kreb, *Chem. Rev.* **104** (2004) 801–824; (b) M.J. Stillman, C.F. Shaw, K.T. Suzuki, John Wiley & Sons: New York, 1992; (c) A.X. Zheng, H.X. Li, K.P. Hou, J. Shi, H.F. Wang, Z.G. Ren, J.P. Lang, *Dalton Trans.* **41** (2012) 2699–2706; (d) T.W. Clarkson, L. Magos, *Crit. Rev. Toxicol.* **36** (2006) 609–662; (e) T.S.B. Baul, I. Longkumer, A. Linden, *J. Organomet. Chem.* **761** (2014) 156–168.
- [2] Y. Sarazin, J.A. Wright, M. Bochmann, *J. Organomet. Chem.* **691** (2006) 5680–5687.
- [3] X.-Y. Tang, R.-X. Yuan, Z.-G. Ren, H.-X. Li, Y. Zhang, J.-P. Lang, *Inorg. Chem.* **48** (2009) 2639–2651.
- [4] M.S. Bhara, T.H. Bui, S. Parkin, D.A. Atwood, *Dalton Trans.* (2005) 3874–3880.
- [5] (a) C.S. Lai, E.R.T. Tiekkink, *CrystEngComm* **5** (2003) 253–261; (b) V. Singh, A. Kumar, R. Prasad, G. Rajput, M.G.B. Drew, N. Singh, *CrystEngComm* **13** (2011) 6817–6826; (c) V. Singh, V. Kumar, A.N. Gupta, M.G.B. Drew, N. Singh, *New. J. Chem.* **38** (2014) 3737–3748; (d) N. Singh, A. Kumar, R. Prasad, K.C. Molloy, M.F. Mahon, *Dalton Trans.* **39** (2010) 2667–2675; (e) V. Kumar, K.K. Manar, A.N. Gupta, V. Singh, M.G.B. Drew, N. Singh, *J. Organomet. Chem.* **820** (2016) 62–69; (f) P.J. Heard, Prog. Inorg. Chem. **53** (2005) 1–69; (g) J.S. Casas, E.E. Castellano, J. Ellena, I. Haiduc, A. Sanchez, R.F. Semeniciu, J. Sordo, *Inorg. Chim. Acta* **329** (2002) 71–78; (h) E.G. —Percastegui, L.N. Zakharov, J.G.A. Rodriguez, M.E. Carnes, D.W. Johnson, *Cryst. Growth Des.* **14** (2014) 2087–2091.
- [6] M.S. Bhara, S. Parkin, D.A. Atwood, *Inorg. Chem.* **45** (2006) 2112–2118.
- [7] P.J. Blower, J.R. Dilworth, *Coord. Chem. Rev.* **76** (1987) 121–185.
- [8] E.L. —Torres, M.A. Mendiola, *J. Organomet. Chem.* **725** (2013) 28–33.
- [9] G. Hogarth, *Prog. Inorg. Chem.* **53** (2005) 71–561.
- [10] E.J. Mensforth, M.R. Hill, S.R. Batten, *Inorg. Chim. Acta* **403** (2013) 9–24.
- [11] E.R.T. Tiekkink, *CrystEngComm* (2020) Advance Article.
- [12] G. Hogarth, *Med. Chem.* **12** (2007) 1202–1215.
- [13] (a) A. Kumar, R. Chauhan, K.C. Molloy, G.K. —Kohn, L. Bahadur, N. Singh, *Chem. Eur. J.* **16** (2010) 4307–4314; (b) V. Singh, R. Chauhan, A. Kumar, L. Bahadur, N. Singh, *Dalton Trans.* **39** (2010) 9779–9788; (c) G. Rajput, M.K. Yadav, M.G.B. Drew, N. Singh, *Inorg. Chem.* **54** (2015) 2572–2579; (d) G. Rajput, M.K. Yadav, T.S. Thakur, M.G.B. Drew, N. Singh, *Polyhedron* **69** (2014) 225–233.
- [14] P. Cassoux, L. Valade, *Inorganic Materials*, John Wiley and Sons, Chichester, 1996.
- [15] A.T. Coomber, D. Beljonne, R.H. Friend, J.L. Bredas, A. Charlton, N. Robertson, A.E. Underhill, M. Kurmoo, P. Day, *Nature* **380** (1996) 144–146.
- [16] T. Okubo, H. Anma, N. Tanaka, K. Himoto, S. Seki, A. Seki, M. Maekawa, T. K-Sowa, *Chem. Commun.* **49** (2013) 4316–4318.
- [17] (a) P. O'Brien, J.H. Park, J. Waters, *Thin Solid Films* **431** (2003) 502–505; (b) Y.S. Tan, A.L. Sudlow, K.C. Molloy, Y. Morishima, K. Fujisawa, W.J. Jackson, W. Henderson, S.N.B.A. Halim, S.W. Neg, E.R.T. Tiekkink, *Cryst. Growth Des.* **13** (2013) 3046–3056.
- [18] R. Saumweber, C. Robl, W. Weignad, *Inorg. Chim. Acta* **269** (1998) 83–90.
- [19] (a) I. G-Orozco, J.G.L-Cortes M.C.O-Alfarro, R.A. Toscano, C. A-Toledano, *Inorg. Chem* **45** (2006) 1766–1773; (b) I. G-Orozco, J.G. L-Cortes, M.C. O-Alfarro, R.A. Toscano, G. P-Carrillo, C. A-Toledano, *Inorg. Chem.* **43** (2004) 8572–8576.
- [20] G. Rajput, M.K. Yadav, M.G.B. Drew, N. Singh, *Dalton Trans.* **44** (2015) 5909–5916.
- [21] (a) C.L. Yadav, G. Rajput, K.K. Bisht, M.G.B. Drew, N. Singh, *Inorg. Chem.* **58** (2019) 14449–14456; (b) C.L. Yadav, G. Rajput, K.K. Manar, K. Kumari, M.G.B. Drew, N. Singh, *Dalton Trans.* **47** (2018) 16264–16278.
- [22] K. Kumari, A.S. Singh, K.K. Manar, C.L. Yadav, V.K. Tiwari, M.G.B. Drew, N. Singh, *New J. Chem.* **43** (2019) 1166–1176.
- [23] R. Fu, S. Xiang, S. Hu, L. Wang, Y. Li, X. Huang, X. Wu, *Chem. Commun.* (2005) 5292–5294.
- [24] (a) W.-Y. Wong, L. Li, J.-X. Shi, *Angew. Chem. Int. Ed.* **42** (2003) 4064–4068; (b) M.R. Haneline, M. Tsunoda, F.P. Gabba, *J. Am. Chem. Soc.* **124** (2002) 3737–3742; (c) H.-P. Zhou, P. Wang, L.-X. Zheng, W.-Q. Geng, J.-H. Yin, X.-P. Gan, G.-Y. Xu, J.-Y. Wu, Y.-P. Tian, Y.-H. Kan, X.-T. Tao, M.-H. Jiang, *J. Phys. Chem. A* **113** (2009) 2584–2590.
- [25] C. Jainik, *Dalton Trans.* (2003) 2781–2804.
- [26] N.L. Rosi, J. Kim, M. Eddaoudi, B. Chen, M. O'Keeffe, O.M. Yaghi, *J. Am. Soc.* **127** (2005) 1504–1518.
- [27] M.A. Beno, H.H. Wang, A.M. Kini, K.D. Carlson, U. Geiser, W.K. Kwok, J.E. Thompson, J.M. Williams, J. Ren, M.-H. Whangbo, *Inorg. Chem.* **29** (1990) 1599–1601.
- [28] H. Mori, I. Hirabayashi, S. Tanaka, T. Mori, Y. Maruyama, *Synth. Met.* **70** (1995) 789–790.
- [29] B.S. Furniss, A.J. Hannaford, P.W.G. Smith, A.R. Tatchell, *Vogel's Textbook of Practical Organic Chemistry*, 5th ed., Pearson: Harlow, 1989.
- [30] Oxford Diffraction, CrysAlis CCD, RED, version 1.711.13, copyright (1995–2003), Oxford Diffraction Poland Sp.
- [31] G.M. Sheldrick, *SHELXS-97*, *Acta Crystallogr A64* (2008) 112–122.
- [32] G.M. Sheldrick, *SHELXL2016-6*, program for crystal structure refinement, *Acta Crystallogr. C71* (2015) 3–8.
- [33] O.V. Dolomanov, I.J. Bourhis, R.J. Gildea, J.A.K. Howard, H. Puschmann, *J. Appl. Crystallogr.* **42** (2009) 339–341.
- [34] C.F. Macrae, I.J. Bruno, J.A. Chisholm, P.R. Edgington, P. McCabe, E. Pidcock, L. Rodriguez-Monge, R. Taylor, J. van de Streek, P.A. Wood, Mercury, *CSD 2*, – New features for the visualization and investigation of crystal structures, *J. Appl. Crystallogr.* **41** (2008) 466–470.
- [35] Gaussian 03, revision C.02, M.J. Frisch, G.W. Trucks, H.B. Schlegel, G.E. Scuseria, M.A. Robb, J.R. Cheeseman, J.A. Montgomery, T. Vreven, K.N. Kudin, J.C. Burant, J.M. Millam, S.S. Iyengar, J. Tomasi, V. Barone, B. Mennucci, M. Cossi, G. Scalmani, N. Rega, G.A. Petersson, H. Nakatsuji, M. Hada, M. Ehara, K. Toyota, R. Fukuda, J. Hasegawa, M. Ishida, T. Nakajima, Y. Honda, O. Kitao, H. Nakai, M. Klene, X. Li, J.E. Knox, H.P. Hratchian, J.B. Cross, V. Bakken, C. Adamo, J. Jaramillo, R. Gomperts, R.E. Stratmann, O. Yazyev, A.J. Austin, R. Cammi, C. Pomelli, J.W. Ochterski, P.Y. Ayala, K. Morokuma, G.A. Voth, P. Salvador, J.J. Dannenberg, V.G. Zakrzewski, S. Dapprich, A.D. Daniels, M.C. Strain, O. Farkas, D.K. Malick, A.D. Rabuck, K. Raghavachari, J.B. Foresman, J.V. Ortiz, Q. Cui, A.G. Baboul, S. Clifford, J. Cioslowski, B.B. Stefanov, G. Liu, A. Liashenko, P. Piskorz, I. Komaromi, R.L. Martin, D.J. Fox, T. Keith, M.A. Al-Laham, C.Y. Peng, A. Nanayakkara, M. Challacombe, P.M.W. Gill, B. Johnson, W. Chen, M.W. Wong, C. Gonzalez, J.A. Pople, Gaussian, Inc., Wallingford CT, 2004.

- [36] GaussView 5.0, Gaussian Inc., Wallingford, CT06492, U.S.A.
- [37] J.S. Casas, M.D. Couce, M.G. -Vega, A. Sanchez, J. Sordo, E.M.V. Lopez, New J. Chem. 40 (2016) 6735–6744.
- [38] (a) A.J. Canty, G.B. Deacon, 1980 Inorg. Chim. Acta, 45 L225–L227; (b) D. Grdenic, Q. Rev, 1965 Chem. Soc., 19 303–328; (c) A. Bondi, 1964 J. Phys. Chem., 68 441–451; (d) J.L. Wardell, Organometallic Compounds of Zinc, Cadmium and Mercury, Chapman and Hall, 1985, pp. 11–129.
- [39] (a) S.R. Tamang, J.-H. Son, J.D. Hoefelmeyer, Dalton Trans 43 (2014) 7139–7145; (b) K.G. von Eschwege, F. Muller, A. Muller, Acta Crystallogr, Sect. E: Struct. Rep. Online 67 (2011) m1858–m1859; (c) A. Castilho, W. Hiller, J. Strahle, J. Bravo, J.S. Casas, M. Gayoso, J. Sordo, J. Chem. Soc. Dalton Trans. (1986) 1945–1948.
- [40] A.W. Addison, T.N. Rao, J. Reedijk, J. van Rijn, G.C. Verschoor, J. Chem. Soc., Dalton Trans. (1984) 1349–1356.
- [41] (a) M. Kasha, Discuss. Faraday Soc. 9 (1950) 14–19; (b) G.N. Lewis, M. Kasha, J. Am. Chem. Soc. 66 (12) (1944) 2100–2116.
- [42] J.C. del Valle, J. Catalan, Phys. Chem. Chem. Phys. 21 (2019) 10061–10069.